Covalent Immobilization of Antibacterial Furanones via Photochemical Activation of Perfluorophenylazide

ARTICLE *in* LANGMUIR · AUGUST 2009

Impact Factor: 4.46 · DOI: 10.1021/la900334w · Source: PubMed

4 AUTHORS, INCLUDING:

Sameer A. Al-Bataineh
University of South Australia
33 PUBLICATIONS **276** CITATIONS
SEE PROFILE

Reto Luginbuehl
Robert Mathys Stiftung Foundation
29 PUBLICATIONS **1,057** CITATIONS
SEE PROFILE

Marcus Textor
ETH Zurich
333 PUBLICATIONS **14,051** CITATIONS
SEE PROFILE

Langmuir
Article
pubs.acs.org/Langmuir

Covalent Immobilization of Antibacterial Furanones via Photochemical Activation of Perfluorophenylazide

Sameer A. Al-Bataineh,*[,†,⊥] Reto Luginbuehl,[‡] Marcus Textor,[†] and Mingdi Yan[§]

[†]*Laboratory for Surface Science and Technology, Department of Materials, ETH Zürich, CH-8093 Hönggerberg, Switzerland,* [‡]*RMS Foundation, CH-2544 Bettlach, Switzerland, and* [§]*Department of Chemistry, Portland State University, PO Box 751, Portland, Oregon 97207.* [⊥]*Current address: Mawson Institute, University of South Australia, Mawson Lakes 5095, Australia*

Received January 27, 2009. Revised Manuscript Received April 1, 2009

N-(3-Trimethoxysilylpropyl)-4-azido-2,3,5,6-tetrafluorobenzamide (PFPA-silane) was used as a photoactive cross-linker to immobilize antibacterial furanone molecules on silicon oxide surfaces. This immobilization strategy is useful, especially for substrates and molecules that lack reactive functional groups. To this end, cleaned wafers were initially incubated in solutions of different concentrations of PFPA-silane to form a monolayer presenting azido groups on the surface. The functionalized surfaces were then treated with a furanone solution followed by illumination with UV light and extensive rinsing with ethanol to remove noncovalently adhered molecules. In the presented study, we demonstrate the ability to control the surface density of the immobilized furanone molecules by adjusting the concentration of PFPA-silane solution used for surface functionalization using complementary surface analytical techniques. The fluorine in PFPA-silane and the bromine in furanone molecules were convenient markers for the XPS study. The ellipsometric layer thickness of the immobilized furanone molecules on the surface decreased with decreasing PFPA-silane concentration, which correlated with a decline of water contact angle as a sign of film collapse. The intensity of characteristic azide vibration in the MTR IR spectra was monitored as a function of PFPA-silane concentration, and the peak disappeared completely after furanone application followed by UV irradiation. As a complementary technique to XPS, TOF-SIMS provided valuable information on the chemical and molecular structure of the modified surfaces and spatial distribution of the immobilized furanone molecules. Finally, this report presents a convenient, reproducible, and robust strategy to design antibacterial coating based on furanone compounds for applications in human health care.

Introduction

The Australian red marine alga *Delisea Pulchra* produces a variety of secondary metabolites known as halogenated furanones. The plant uses these compounds to prevent fouling by micro- and macro-organisms in marine environments. The furanone derivatives are encapsulated in vesicles in specialized gland cells and located both in the interior and on the surface of the plant. The total surface concentration of the most abundant furanone compounds produced by the plant ranges between 100 and 500 ng cm^{-2}.[1−3] Furanone compounds protect the plant against micro- and macrofoulers as well as pathogenic bacteria.[4−7] These secondary metabolites inhibit bacterial adhesion and biofilm development through interference with the quorum sensing pathways in gram-negative and gram-positive bacteria, including human pathogens, a mechanism that has so far never resulted in bacterial resistance.[4,8−11] As nosocomial medical device infections often have severe consequences and there is a lack of successful long-term preventative strategies, these compounds become highly attractive as promising antibacterial molecules for use in human health care, for example as antibacterial coatings on medical devices and implants.[12,13]

In order to ensure effectiveness and stability for extended periods of time, these compounds should be immobilized covalently on a surface. In our study, we used a perfluorophenylazide-functionalized silane (PFPA-silane) photolinker utilizing the azide functionality for light-induced immobilization of the furanone. This immobilization method is simple and reproducible and has been proven to be efficient to immobilize polymers and biomolecules on silicon oxide surfaces.[14,15] In general, this immobilization strategy is considered very attractive for immobilizing molecules, such as nonfunctionalized furanones, that do not possess any suitable functional group for immobilization via conventional chemical reactions. In addition, perfluorophenyazides have significantly higher CH and NH insertion efficiencies compared to their non-fluorinated analogues, and therefore, they

*Author for correspondence: e-mail Sameer.Al-Bataineh@unisa.edu.au, Tel +61 8 8302 3072, Fax +61 8 8302 5689.

(1) de Nys, R.; Givskov, M.; Kumar, N.; Kjelleberg, S.; Steinberg, P. D. *Prog. Mol. Subcell. Biol.* **2006**, *42*, 55–86.
(2) de Nys, R.; Dworjanyn, S. A. *Mar. Ecol.: Prog. Ser.* **1998**, *162*, 79–87.
(3) Dworjanyn, S. A.; de Nys, R.; Steinberg, P. D. *Mar. Biol.* **1999**, *133*, 727–736.
(4) Manefield, M.; de Nys, R.; Kumar, N.; Read, R.; Givskov, M.; Steinberg, P.; Kjelleberg, S. *Microbiology* **1999**, *145*, 283–291.
(5) de Nys, R.; Steinberg, P. D.; Willemsen, P.; Dworjanyn, S. A.; Gabelish, C. L.; King, R. J. *Biofouling* **1995**, *8*, 259–271.
(6) Maximilien, R.; de Nys, R.; Holmstrom, C.; Gram, L.; Givskov, M.; Crass, K.; Kjelleberg, K.; Steinberg, P. *Aquat. Microb. Ecol.* **1998**, *15*, 233–246.
(7) Wright, J. T.; de Nys, R.; Poore, A. G. B.; Steinberg, P. D. *Ecology* **2004**, *85*, 2946–2959.
(8) Givskov, M.; de Nys, R.; Manefield, M.; Gram, L.; Maximilien, R.; Eberl, L.; Molin, S.; Steinberg, P. D.; Kjelleberg, S. *J. Bacteriol.* **1996**, *178*, 6618–6622.
(9) Manefield, M.; Rasmussen, T. B.; Henzter, M.; Andersen, J. B.; Steinberg, P.; Kjelleberg, S.; Givskov, M. *Microbiology* **2002**, *148*, 1119–1127.
(10) Ren, D.; Sims, J. J.; Wood, T. K. *Environ. Microbiol.* **2001**, *3*, 731–736.
(11) Ren, D.; Bedzyk, L. A.; Setlow, P.; England, D. F.; Kjelleberg, S.; Thomas, S. M.; Ye, R. W.; Wood, T. K. *Appl. Environ. Microbiol.* **2004**, *70*, 4941–4949.
(12) Read, R.; Kumar, N.; Wilcox, M.; Zhu, H.; Griesser, H. J.; Thissen, H.; Muir, B.; Hughes, T. EP1296673, 2003.
(13) Hume, E. B. H.; Baveja, J.; Muir, B.; Schubert, T. L.; Kumar, N.; Kjelleberg, S.; Griesser, H. J.; Thissen, H.; Read, R.; Poole-Warren, L. A. *Biomaterials* **2004**, *25*, 5023–5030.
(14) Pei, Z.; Yu, H.; Theurer, M.; Waldén, A.; Nilsson, P.; Yan, M.; Ramström, O. *ChemBioChem* **2007**, *8*, 166–168.
(15) Liu, L.; Engelhard, M. H.; Yan, M. *J. Am. Chem. Soc.* **2006**, *128*, 14067–14072.

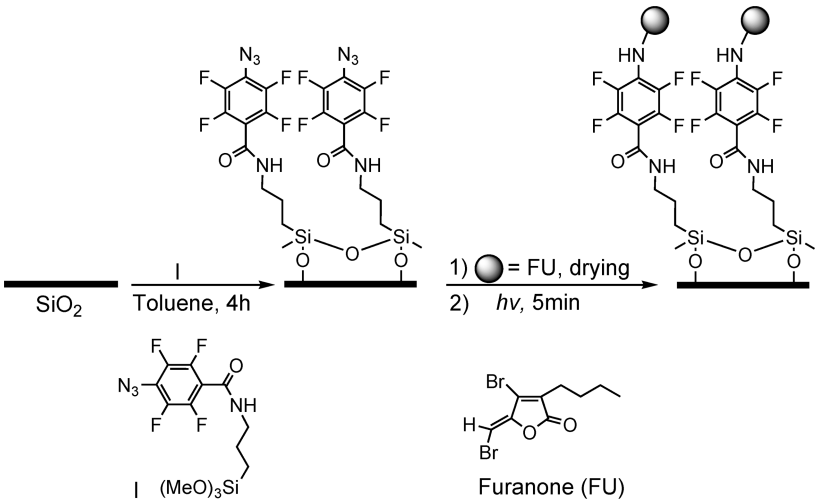

Figure 1. Covalent immobilization of furanone molecules on PFPA-functionalized surface.

are considered an important class of photoaffinity labeling reagents.[16]

In our study, we aimed at using a PFPA-silane photolinker for the covalent immobilization of nonfunctionalized antibacterial furanone compounds onto silicon oxide surfaces and to control the surface density through adjustment of the PFPA solution concentration. The surfaces were characterized extensively by XPS and ToF-SIMS at each stage of the surface modification procedure. The results of microbiological studies will be communicated in a future separate publication.

Experimental Section

Materials. The furanone compound used in our study, abbreviated as FU, was 3-butyl-4-bromo-5-(bromomethylene)-2(5*H*)-furanone; it was synthesized according to published protocols.[17,18] We report here the NMR data for the compound acquired on a Varian Gemini Fourier Transform NMR spectrometer (300 MHz, $CDCl_3$) δ (ppm): 0.96, t, J 7.2 Hz, $CH_2CH_2CH_2CH_3$; 1.38, m, $CH_2CH_2CH_2CH_3$; 1.58, m, $CH_2CH_2CH_2CH_3$; 2.38, t, J 7.2 Hz, $CH_2CH_2CH_2CH_3$; 6.27, s, CHBr. *N*-(3-Trimethoxysilylpropyl)-4-azido-2,3,5,6-tetrafluorobenzamide (PFPA-silane) was synthesized adapting previously published protocols.[16,19] Water used in the contact angle measurements was of ultrapure quality (Millipore Milli-Q system) with at least 18.2 MΩ resistivity. All chemicals and solvents used in this study either for synthesis or surface modification were of at least ACS reagent grade and used as received without further purification.

Surface Modification. Silicon wafers with ~2.3 nm native oxide layer (WaferNet GmbH, Germany) were cut into 1 × 1 cm size and cleaned in piranha solution (7:3 v/v concentrated H_2SO_4/35 wt % H_2O_2) for 1 h at 80−90 °C, then washed thoroughly with boiling water for another 1 h, and dried under a stream of nitrogen. *Caution! Piranha solution reacts violently with many organic compounds; use extreme care when handling it*. The cleaned wafers were soaked in toluene containing PFPA-silane at concentrations ranging from 2.5 to 3 × 10^{-3} mM for 4 h at room temperature and under dark conditions. This process was carried out in sealed vials to minimize contact with moisture in the air. The treated wafers were rinsed with toluene then ethanol, dried under nitrogen, and then allowed to cure at room temperature for 24 h. A 40 μL of furanone compound solution (1 mg/mL in EtOH) was applied to the prepared PFPA-silane surfaces, and the samples were left overnight to have complete evaporation of the solvent—all operations were carried out under dark conditions. Subsequently, the samples were irradiated for 5 min with 280 nm light at ~36 mW cm^{-2} (at 15 cm distance from the lamp) using a medium-pressure Hg lamp (ACE Glass Incorporation) with 280 nm optical filter (Scott AG, Switzerland). Finally, unbound furanone molecules were removed by washing the samples gently with ethanol. The modified surface was then dried under stream of nitrogen. The prepared surfaces were stored in cleaned containers until analysis. Figure 1 shows the schematic illustration of the immobilization process.

X-ray Photoelectron Spectroscopy (XPS). XPS analysis was performed using a Sigma probe instrument (Thermo Electron Corp., UK) equipped with a nonmonochromatic Al Kα ($h\nu$ = 1486.6 eV) source at a power of 300 W. The pass energy for survey spectra was 50 eV with 1 eV step size and for high-resolution spectra of individual elements 25 eV with 0.1 eV step size, respectively. The base pressure in the main chamber during analysis was ≤10^{-9} mbar. The spectra were acquired at an emission angle of 90°. Elements present on the surface were identified from survey spectra and quantified in the high-resolution spectra. Atomic compositions (in at. %) were calculated using CasaXPS Software (version 2.3.12, www.casaxps.com) by determining the relevant integral peak intensities using a nonlinear Shirley-type background and applying the sensitivity factors of Scofield.[20] In order to minimize X-ray-induced sample degradation, the time of exposure to X-ray irradiation was kept to the minimum required to record an adequate signal-to-noise ratio. Charging effects of the samples during analyses were corrected using a reference value of 285.0 eV for the binding energy of the main C 1s component arising from neutral hydrocarbon (CHx).[21] At least three samples were analyzed of each modification type, and the average was calculated. CasaXPS software was also used to separate the component peaks in the high-resolution spectra. The line shape of the curves was assumed to be Gaussian−Lorentzian with a 30% Lorentzian component. The Gaussian−Lorentzian mixing ratio and peak width (full width at half-maximum, fwhm) were constrained to have the same value for all components.

Time-of-Flight Secondary Ion Mass Spectrometry (TOF-SIMS). Spectra were acquired using TOF-SIMS V from ION TOF (Germany). The device was equipped with a reflectron TOF analyzer with a mass range of 0−10 000 m/z. All spectra were

(16) Keana, J. F. W.; Cai, S. X. *J. Org. Chem.* **1990**, *55*, 3640–3647.
(17) Beechan, C. M.; Sims, J. J. *Tetrahedron Lett.* **1979**, *20*, 1649–1652.
(18) Manny, A. J.; Kjelleberg, S.; Kumar, N.; de Nys, R.; Read, R. W.; Steinberg, P. *Tetrahedron* **1997**, *53*, 15813–15826.
(19) Yan, M.; Ren, J. *Chem. Mater.* **2004**, *16*, 1627–1632.
(20) Scofield, J. H. *J. Electron Spectrosc. Relat. Phenom.* **1976**, *8*, 129–137.
(21) Beamson, G.; Briggs, D. *High Resolution XPS of Organic Polymers*; John Wiley and Sons: Chichester, 1992.

Table 1. XPS Results of FU-Functionalized Surfaces (Values in Parentheses Represent SD)

		atomic concentration [%]					
sample	concentration [mM][a]	C	N	F	O	Si	Br
FU/PFPA-silane/SiO_2	2.50	23.9 (0.6)	2.9 (0.1)	3.7 (0.2)	25.3 (0.7)	43.7 (0.9)	0.59 (0.11)
FU/PFPA-silane/SiO_2	1.26	22.6 (0.5)	2.7 (0.0)	3.5 (0.1)	25.4 (0.1)	45.3 (1.1)	0.41 (0.01)
FU/PFPA-silane/SiO_2	0.025	10.8 (0.0)	1.0 (0.1)	1.2 (0.2)	26.8 (1.2)	60.1 (1.6)	0.14 (0.04)
FU/PFPA-silane/SiO_2	0.006	10.0 (1.3)	0.7 (0.2)	0.7 (0.1)	27.7 (1.5)	60.8 (2.6)	0.10 (0.04)
FU/PFPA-silane/SiO_2	0.003	7.3 (0.1)	0.5 (0.0)	0.5 (0.0)	27.3 (0.2)	64.3 (0.4)	0.11 (0.01)

[a] PFPA-silane solution concentration used for surface functionalization.

recorded using pulsed Bi^{3+} primary ions (0.9 ns pulse length, 0.6 pA pulsed ion current) with a total ion dose of $\sim 10^{12}$ ions/cm^2 per spectrum. The analyzed area was fixed to $150 \times 150\ \mu m^2$ and a lateral resolution of $\sim 10\ \mu m$ for all spectra. A mass resolution $m/\Delta m$ of $\sim$8000 at nominal m/z 41 amu ($C_3H_5^+$) and m/z 36 amu (C_3^-) was typically achieved in the positive- and negative-ion mode, respectively. A minimum of two samples with five points per sample were analyzed for each sample type.

Variable Angle Spectroscopic Ellipsometry (VASE). The dry thicknesses of PFPA-silane and FU/PFPA-silane adlayers were determined by VASE (M-2000F, LOT Oriel GmbH, Germany). Measurements were conducted under ambient conditions at three angles of incidence (65°, 70°, and 75°) in the spectral range of 370−1000 nm. Spectroscopic scans were taken after every step (after cleaning, PFPA-silane adsorption, and FU immobilization). Three samples were analyzed for each type of modification, and the results were averaged. Measurements were fitted with the WVASE32 analysis software using a multilayer model for an oxide layer on silicon and an organic adlayer (PFPA-silane and FU). The n and k values for the oxide layers were fitted, and the adlayer thickness for both the PFPA-silane and FU was determined using a Cauchy model.

Water Contact Angle Measurements. The surface hydrophilicity of the PFPA-silane and FU/PFPA-silane was characterized by measuring static water contact angles, θ_w, by employing a contact-angle goniometer (Ramé-Hart model 100). Three samples were analyzed for each type of modification, and the results were averaged.

Multiple Transmission and Reflection (MTR) IR Spectroscopy. Infrared spectra were collected with multiple transmission and reflection (MTR) measurement using a homemade accessory on a Bruker IFS66/S instrument at 4 cm^{-1} resolution.[22] Double side polished silicon substrate (30 mm × 18 mm) was placed between two gold mirrors. The sensitivity could be increased by multiple transmissions, and reflections occurred between the two mirrors. The angle of incidence was adjusted to be around 74°, and mirror distance is 2 mm. A grid polarizer was installed in the light path between the source and the sample. A precleaned wafer with piranha solution was used as background.

Results and Discussion

In this study, we followed an approach to control the density of furanone molecules immobilized on the surface by adjusting the concentration of the photolinker (i.e., PFPA-silane) used for surface functionalization. Functionalization was obtained by sequential treatment of cleaned Si-wafer with the silane solution, curing for 24 h, addition of furanone, and UV irradiation. Then the surfaces were rinsed with ethanol to remove unbound furanone molecules.

The immobilization of PFPA-silane was monitored by XPS in order to ensure that the modification step occurred successfully. Immobilization of the silane was followed by quantification of the fluorine signal of the PFPA-silane while UV activation of the azide functionality was observed in the nitrogen signal and the appearance of bromide signal from the immobilized furanone. The collected XPS data of the furanone-functionalized surfaces are summarized in Table 1. The atomic concentration (%) of Br from furanone molecules present on the surface decreased with decreasing PFPA-silane concentration (Table 1), demonstrating the ability to control consistently the PFPA surface concentration.

It is important to ascertain that the furanone molecules are indeed covalently immobilized on the PFPA-functionalized surface and not just physically adsorbed, as they may not maintain extended antibacterial activity if they leach from the surface, which could cause adverse effects on sensitive tissues. We tested the capacity of furanone molecules to undergo physisorption on the functionalized silicon oxide surface by carrying out the same procedure but omitting UV irradiation. This control test led to complete removal of furanone molecules in the ethanol washing step, as demonstrated by the absence of a bromine signal in the XPS survey spectrum (data not shown).

The presence of F atom in the PFPA-silane adlayer proved to be a useful XPS marker to monitor the changes in the photolinker surface density. The intensity of the high-resolution F 1s peak, reflecting the density of the photoactive groups present on the surface, increased with increasing PFPA-silane concentration (Figure 2a). The surface density of the PFPA-silane molecules, represented by the atomic concentration (%) of F (Figure 2b), reached a plateau for PFPA-silane concentration larger than 1 mM, which was interpreted as formation of a saturated full monolayer.

To demonstrate the presence of azido groups on the PFPA-functionalized surfaces, a high-resolution XPS N 1s spectrum was curve-fitted, and the results are presented in Figure 3. Four distinct N 1s peaks associated with the azide and amide functionalities were resolved at binding energies (BEs) of 399.3, 400.8, 401.4, and 404.3 eV. The peak at 404.3 eV is attributed to the central nitrogen of the azide functionality (N_b) because of its low electron density relative to the other two terminal nitrogen atoms. The peak at 401.4 eV is attributed to nitrogen atom of the azide associated with the fluorobenzene ring (N_a) and the peak at 399.3 eV to the terminal nitrogen atom of the azide (N_c). In addition, the peak at 400.8 eV is assigned to the amide nitrogen (N_d). Furthermore, the additional area under the peaks of (N_a) and (N_d) is believed to be from the contribution of the nitrogen atoms of tetrafluoroazacycloheptatetrane. This derivative can be formed as a result of ring expansion of the (singlet) tetrafluorophenylnitrene intermediate after losing N_2, a result of azide decomposition due to X-ray exposure during analysis. More information on the photolysis scheme of the arylazides can be found in Poe et al.[23] and Brunner.[24]

(22) Liu, H.-B.; Venkataraman, N. V.; Bauert, T. E.; Textor, M.; Xiao, S.-J. *J. Phys. Chem. A* **2008**, *112*, 12372–12377.

(23) Poe, R.; Schnapp, K.; Young, M. J. T.; Grayzar, J.; Platz, M. S. *J. Am. Chem. Soc.* **1992**, *114*, 5054–5067.

(24) Brunner, J. *Annu. Rev. Biochem.* **1993**, *62*, 483–514.

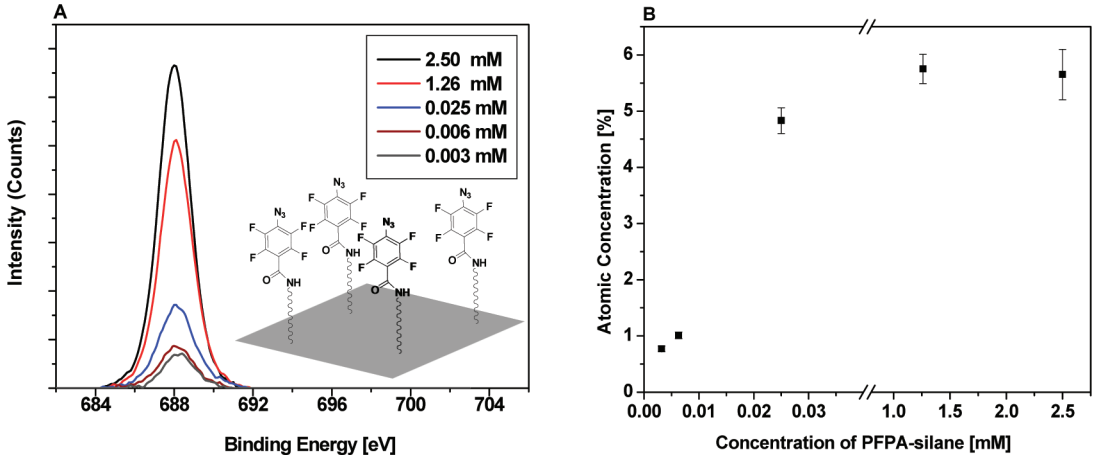

Figure 2. Change in the XPS intensity of the F 1s peak (A) and fluorine concentration (%) (B) as a function of PFPA-silane concentration [mM].

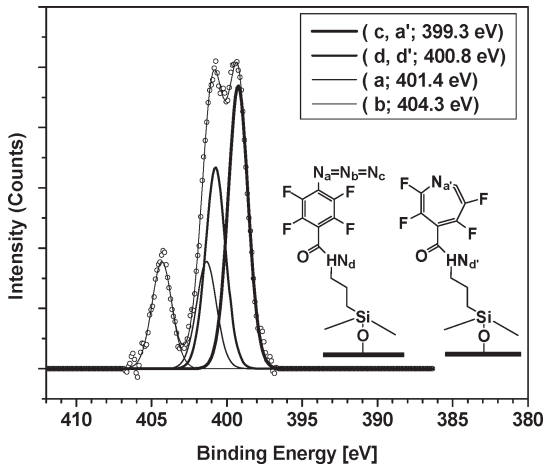

Figure 3. Curve-fitting of the XPS N 1s region acquired after PFPA-silane immobilization. The four components were constrained to same full width at half-maximum (fwhm) (1.6 eV). The intensity of the four components reflects contributions from both the different azide and the amide nitrogen.

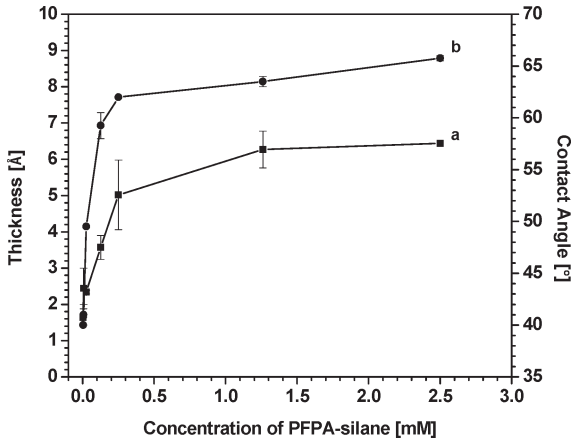

Figure 4. Thickness, measured by ellipsometry (line a), and water contact angle (line b) after furanone immobilization as a function of PFPA-silane concentration.

The thickness and static water contact angle of the furanone-functionalized surfaces were measured and plotted against the concentration of PFPA-silane solution (Figure 4). The surface density of furanone molecules increases with increasing PFPA-silane solution concentration as indicated by the increase in the ellipsometric layer thickness upon furanone immobilization (Figure 4, line a). At the highest concentration of the PFPA-silane (2.5 mM), the layer thickness of the immobilized furanone molecules was ~0.7 nm and the water contact angle was found to be ~65° (Figure 4, line b). Whereas, at the lowest concentration (3×10^{-3} mM) the thickness declined to ~0.2 nm and the water contact angle dropped to ~40°, indicating the lower surface density of the immobilized (hydrophobic) furanone.

Infrared spectroscopy (IR) was used as a complementary analytical technique to characterize the functionalized surfaces. Multiple transmission and reflection (MTR) spectra for various concentrations of PFPA-silane solutions immobilized on a double-side polished silicon wafer are depicted in Figure 5a. The spectra contain peaks arising from azide (asymmetric stretching, 2126 cm^{-1}), amide (stretching for amide I, 1650 cm^{-1} and bending for amide II, 1558 cm^{-1}), and phenyl ring (stretching from C=C, 1488 cm^{-1}) functionalities. We observed that the peak area of the azide functionality decreased as a result of PFPA-silane dilution, reflecting the decrease in the surface density of the photoactive groups and subsequently immobilized furanone. A complete photodecomposition of the azide species occurred upon irradiation, as demonstrated by the disappearance of the corresponding azide peak at 2126 cm^{-1} (Figure 5b).

To provide more detailed information on the molecular structure of the outermost surface layer, positive and negative TOF-SIMS spectra were acquired on clean SiO_2, PFPA-silane/SiO_2, and FU/PFPA-silane/SiO_2 surfaces. The concentration of PFPA-silane solution used for surface functionalization was 1.26 mM. The full spectra are not shown in this report. Careful analysis of the acquired spectra, within the mass region 0−500 m/z, of the PFPA-silane functionalized surfaces revealed characteristic fragment ions that could be assigned to molecular species present mainly in the positive spectra; those fragment ions are reported in Table 2. The positive fragment ion at m/z = 162 had higher intensity compared to the other fragments. The detection of this fragment ion is consistent with the findings from the XPS results, indicating that the azide moiety was partially decomposed during both XPS and TOF-SIMS analyses. Interestingly, the positive fragment ion at m/z = 218 represents a molecular species that carries the azide functionality, demonstrating the presence of the photoactive groups at the outermost surface. No strong characteristic fragment ions assignable to molecular species associated with the furanone compound were detected. However, the negative TOF-SIMS spectra contained

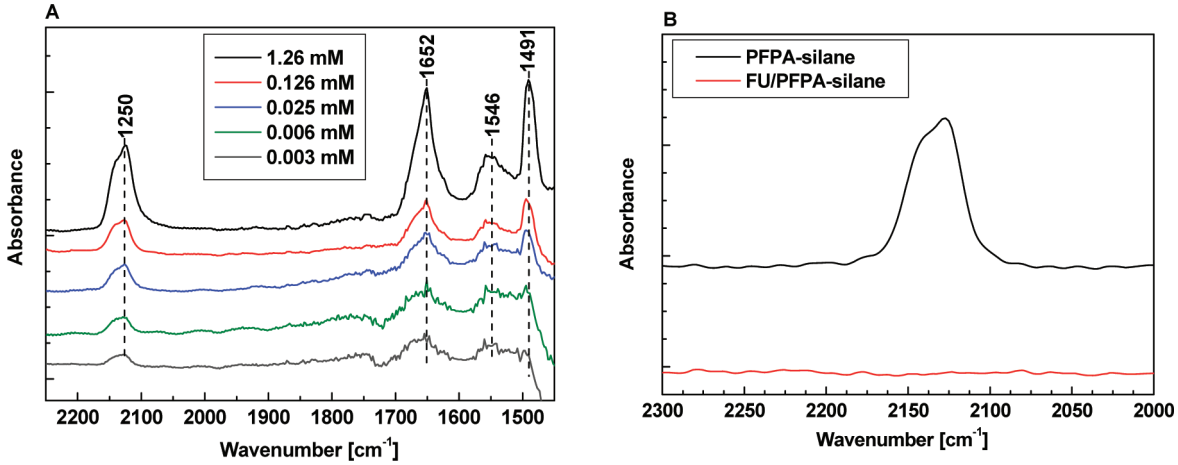

Figure 5. MRT IR spectra showing (A) the change in the azide peak intensity as a function of PFPA-silane concentration and (B) the disappearance of the azide peak upon UV irradiation and concomitant furanone coupling.

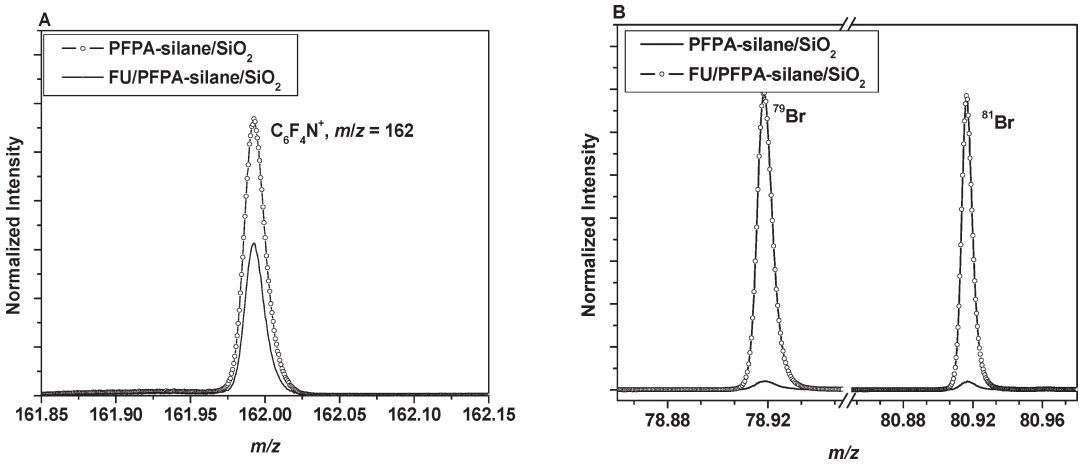

Figure 6. Normalized overlay positive TOF-SIMS spectra in the mass range m/z = 161.85−162.15 (A) and negative TOF-SIMS spectra in the mass range m/z = 78.85−81.15 (B) before and after furanone immobilization.

Table 2. Characteristic Peaks in the Positive Ion TOF-SIMS Spectra of the PFPA-Silane

Nominal Mass [m/z]	Chemical Formula	Possible Structure
162	$C_6F_4N^+$	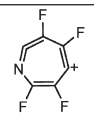
190	$C_7F_4NO^+$	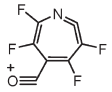
218	$C_7F_4N_3O^+$	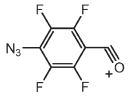

several fragment ions characteristic for the furanone compound such as CO_2^- (m/z = 44) and Br^- isotopes (m/z = 79, 81, 158, 160, 162). Figure 6a shows the changes in the normalized intensity of the positive fragment ion $C_6F_4N^+$ (m/z = 162) before and after furanone immobilization, whereas Figure 6b shows the appearance of bromine peaks (^{79}Br and ^{81}Br) in the negative TOF-SIMS spectra of the surface upon furanone immobilization.

The spatial distribution of the PFPA-silane was monitored utilizing the imaging mode of the TOF-SIMS. The acquired images from raw data of the characteristic positive fragment ions (data not shown) reveal fairly homogeneously distribution across the analyzed area (150 × 150 μm). Given the lateral resolution in the ToF-SIMS images of ~10 μm, we can conclude that there are no larger defects present in the coatings.

Conclusions

We have presented a versatile strategy to design antibacterial coating using furanone compounds. The density of the immobilized furanone on the surface was controlled by adjusting the concentration of the PFPA-silane solution used for surface functionalization. The changes in surface density of the PFPA-functionalized surfaces were monitored by XPS, and the results showed that a saturated monolayer was reached at concentrations higher than 1 mM. The furanone molecules were covalently immobilized on the surface as indicated by the presence of bromine signals unique to furanone compound in the XPS survey spectra and by the fact that no bromine signal was detected when the UV photoactivation step was omitted. Further analysis of the XPS data by means of curve fitting showed the presence of tetrafluoroazacycloheptatetrane intermediate on the surface,

indicating that the azide groups of the immobilized PFPA-silane partially decomposed in the X-rays beam during analysis. The ellipsometric layer thickness of the immobilized furanone for the various surface densities of PFPA-silane was in the nanometer range. Consistent with the XPS data, the MTR IR spectra showed peaks characteristic for the azide and amide functionalities of the immobilized PFPA-silane. The azide peaks disappeared upon UV irradiation. Characteristic fragment ions were found in the positive TOF SIMS spectra acquired on the PFPA-silane surfaces. After furanone immobilization no characteristic fragment ions were found in the positive TOF SIMS spectra; however, furanone-related bromine was detected in the negative TOF SIMS spectra.

The qualitative and quantitative surface analytical data presented in this report are expected to provide valuable information for the planned investigation of antimicrobial activity in vitro and in vivo.

Acknowledgment. The authors gratefully acknowledge the financial support made available by Dr. h.c. Robert Mathys Foundation, Switzerland. We thank Dr. Hong-Bo Liu for access to the MTR IR setup for IR measurements. We also thank Dr. Karl-Emanuel Mayerhofer and Dr. Beat Keller, Empa, Switzerland, for their help with TOF-SIMS measurements. M. Yan acknowledges financial support from Swiss National Science Foundation, and NIH under Award Numbers R01GM080295 and 2R15GM066279.